Available online at www.sciencedirect.com
SCIENCE DIRECT®
ELSEVIER
European Journal of Mechanics B/Fluids 22 (2003) 73–84

An iterative procedure for solving mixed convection boundary layers with reverse flows

Mustapha Amaouche, Bachir Meziani

Laboratoire de physique théorique, Université de Béjaia, route de Targua Ouzemmour, 06000 Béjaia, Algérie

Received 15 October 2001; received in revised form 15 May 2002; accepted 22 October 2002

Abstract

The absence of Cauchy conditions to characterize the beginning of the boundary layer in asymmetric mixed convection flow around a heated horizontal cylinder makes it impossible to study by a direct method the stagnation zone independently of the remaining part of the flow. This difficulty is due to the upstream–downstream interaction owing to the occurrence of ascending buoyancy-driven flow near the wall and descending flow far away from the wall. If the far stream effects are small compared to the buoyancy forces, a second order asymptotic expansion leads to a semi-analytical solution valid in the vicinity of the free convection stagnation point. The latter provides the starting conditions for the boundary layer. An iterative method based upon some variational concepts is then implemented in order to numerically integrate the boundary layer equations in the region where reverse flow occurs. Some numerical results are finally presented to show the influence of the transverse stream on some characteristics of the boundary layer.

Keywords: Iterative procedure; Mixed convection; Variational method; Reverse flow; Boundary layer

1. Introduction

In this paper we are concerned with the asymmetric mixed convection flow over a heated horizontal cylinder placed in a nonvertically oriented free stream. The most characteristic feature of this problem is perhaps the fact that the location of the stagnation point, which is somewhere between the stagnation points of free and forced convection, is not known in advance. Therefore, the associated Cauchy conditions which characterize the starting of the boundary layer are no longer known. This results from the downstream–upstream interaction which is due to the occurrence of a reverse flow in the region between the stagnation points of free and forced convection, where the sources of motion are opposite. These obvious reasons make the problem fundamentally different from the symmetric configuration where the free stream is directed vertically. In the latter case, the stagnation point occurs at the lowest (or uppermost) point of heated (or cooled) cylinder.

The literature on symmetric mixed convection is relatively extensive. In the high Reynolds and Grashof numbers range, Joshi and Sukhatme [1] and Sparrow and Lee [2] looked at the boundary layer flow induced by a vertical stream over a heated circular cylinder. The solution is obtained by expanding velocity and temperature profiles in power series in x which is the coordinate that measures the distance from the lowest point of the cylinder. The first term of the expansion is a similarity solution which describes the local behaviour of the boundary layer in the vicinity of the stagnation point. It is shown that at this point both natural and forced convection are important. Merkin [3] extended the solution of the problem discussed in [1,2] by numerical computation. He found that heating the cylinder delays separation of the flow and can suppress it completely if the cylinder is warm enough. Cooling the cylinder leads to the inverse effect and for a sufficiently cooled cylinder, the boundary layer is removed. In the low Reynolds and Grashof numbers limit, the incipient effects of buoyancy were investigated by Wood [4]

E-mail addresses: m_amaouche@yahoo.fr (M. Amaouche), bachirdidih@hotmail.com (B. Meziani).

0997-7546/03/$ – see front matter
doi:10.1016/S0997-7546(02)00004-3

mainly with series expansion. Theoretical correlations of the heat transfer when there is dominance of either one of forced or free convection over the other are given by Nakai and Okazaki [5] by the method of matching the solutions in the inner and outer regions. For the range of intermediate Reynolds and Grashof numbers, the symmetric mixed convection from circular cylinder was numerically studied by Badr [6] and Sunden [7].

Except for a few particular configurations such as those discussed above, the location of the stagnation point is in general unknown, so the incipient structure of the boundary layer cannot be easily determined. This is the case of mixed convection from a heated or cooled cylinder when the corresponding stagnation points of the potential flow and free convection do not coincide, as is the case when the far stream is inclined by some angle α with respect to the vertical line. Only limited data concerning the influence of this factor exist in the literature. Wood [4] discussed further the incipient effect on the slanted upward basic flow at an acute angle α to the vertical line by putting $\mathrm{Gr}\cos\alpha$ instead of Gr and estimated the change in pressure across the wake. This problem is also examined by Nakai and Okazaki [5] where theoretical solutions are given for the case when either the forced or free convection is subordinate to the other. In the range of intermediate Reynolds and Grashof numbers, numerical results obtained by Badr [8], Amaouche and Peube [9] showed that the angle α has an appreciable effect on both local and global characteristics of the flow. In the experiments performed by Hatton et al. [10], it was attempted to express the Nusselt number as a vectorial sum of the forced and free convective heat transfer correlation; this concept seems, however, to be irrelevant except for the case of symmetric flow. When the Reynolds and Grashof numbers are relatively large, there are a few studies about the heat transfer from a cylinder by asymmetric mixed convection. Only measurements on the average heat transfer coefficient are available (see Sharma and Sukhtame [11], Oosthuizen and Madan [12]. For this range of parameters, the flow is governed by the boundary layer equations whose solution depends on the structure of the incipient boundary layer at the stagnation point. The latter is located somewhere between the stagnation point of the potential flow and the lowest point of the cylinder. In the vicinity of this point, the flow structure looks like that of a separated flow. This is related to the fact that buoyancy forces act locally as an increasing adverse pressure gradient. Because both the position of the stagnation point and the conditions characterizing the beginning of the boundary layer are unknown a priori, it is not possible to study the stagnation zone independently of the remainder of the flow. This interaction is caused by the reversal of the flow direction. Formally, this difficulty may be translated into the coupling of different functions when representing the flow in the Blasius series (see Amaouche [13]). To overcome this difficulty without losing the boundary layer character, looking for appropriate models which take into account the elliptic nature of the problem appears to be necessary. It has been possible to recover the Cauchy conditions associated with the beginning of the boundary layer when buoyancy forces are sufficiently weak compared to the external pressure gradient (see Amaouche and Nouar [14]). The other limiting case where the flow is dominated mainly by free convection is considered in the present study. First, an asymptotic approximation is developed in order to describe the stagnation point flow. Because of the upstream influence originating from the coexistence of ascending and descending flow in the opposite mixed convection region, a direct integration of the boundary layer equations fails to converge. In order to resolve this difficulty, the boundary layer equations are separately integrated on each side of the curve along which the longitudinal component of the velocity vanishes. It is however assumed, in accordance with our approach of weakly perturbed free convection boundary layer flow, that the boundary layer thickness remains a well defined function along the surface and the first approximation to the external flow therefore remains the classical potential flow past the geometrical body.

2. Governing equations

Under the combined effects of the outer flow, the external pressure gradient and buoyancy forces, a boundary layer flow takes place, starting from the stagnation point whose location is a priori unknown. The latter is however situated between the stagnation points of potential flow and free convection. The flow is assumed to be steady and two dimensional. To illustrate this, a horizontal uniformly heated cylinder is considered. The free stream direction is inclined by a variable angle α with respect to the vertical line. With the stated assumptions and the Boussinesq approximation, the governing boundary layer equations are, in dimensionless form:

$$u_x + v_y = 0, \tag{1}$$

$$uu_x + vu_y - u_{yy} - T\sin x = u_e \frac{\mathrm{d}u_e}{\mathrm{d}x}, \tag{2}$$

$$\mathrm{Pr}(uT_x + vT_y) - T_{yy} = 0. \tag{3}$$

These equations are subject to the boundary conditions:

$$u(x,0) = v(x,0) = 0, \qquad T(x,0) = 1, \tag{4}$$

$$u(x,\infty) = u_e(x), \qquad T(x,\infty) = 0. \tag{5}$$

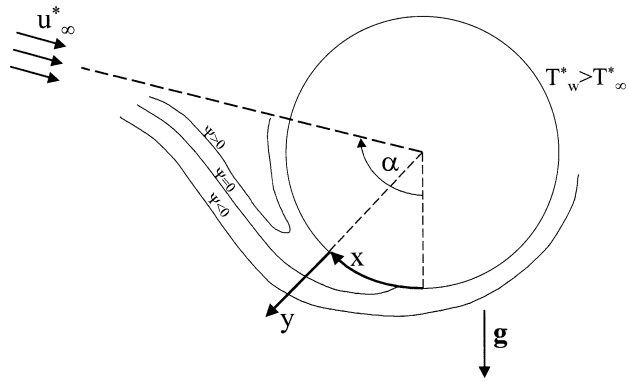

Fig. 1. Sketch of the problem.

Introducing the stream function Ψ defined from the velocity by $(u, v) = (\Psi_y, -\Psi_x)$, Eqs. (1)–(3) take the more convenient form:

$$L\Psi_y - \Psi_{yyy} - T\sin x = u_e \frac{\mathrm{d}u_e}{\mathrm{d}x}, \tag{6}$$

$$\mathrm{Pr}\, LT - T_{yy} = 0 \tag{7}$$

with the boundary conditions for Ψ:

$$\Psi(x,0) = \Psi_y(x,0) = 0, \qquad \Psi_y(x,\infty) = u_e(x), \tag{8}$$

where L abbreviates the convective operator $\Psi_y\partial_x - \Psi_x\partial_y$. Because of the prominence of free convection, the scaling factors are naturally connected to the Grashof number $\mathrm{Gr} = g\beta(T_w^* - T_\infty^*)R^3/\nu^2$ where g, β, ν, R, T_w^* and T_∞^* denote gravitational acceleration, thermal expansion coefficient, kinematics viscosity, radius of the cylinder, dimensioned constant temperatures of the wall and at infinity respectively. In order that the dimensionless variables be of order unity in the boundary layer, the radial coordinate y, measured from the surface, is nondimensionalized by $R\mathrm{Gr}^{-1/4}$ and the stream function Ψ by $\nu\mathrm{Gr}^{1/4}$. Therefore, the angular and radial velocity components are scaled by $\nu\mathrm{Gr}^{1/2}/R$ and $\nu\mathrm{Gr}^{1/4}/R$ respectively. The function u_e indicates the potential flow velocity along side the cylinder. Expressed in dimensionless form, it is written $u_e(x) = \mathrm{Re}\,\mathrm{Gr}^{-1/2}\sin(x-\alpha)$ where x is the angular variable whose origin is the free convection stagnation point and $\mathrm{Re} = 2u_\infty^* R/\nu$ stands for the Reynolds number; u_∞^* being the dimensioned velocity of the uniform free stream. T indicates the dimensionless temperature which is related to the dimensioned temperature T^* by $T = (T^* - T_\infty^*)/(T_w^* - T_\infty^*)$. Besides the inclination α and the parameter $\varepsilon = \mathrm{Re}\,\mathrm{Gr}^{-1/2}$ which characterizes the smallness of the free stream effects compared to the buoyancy effects, the problem also depends on the Prandtl number $\mathrm{Pr} = \nu/\gamma$ where γ designates the coefficient of thermal diffusivity. The schematic of the problem is shown in Fig. 1.

3. Stagnation point flow

In the following, we assume that the relative magnitude of forced convection is sufficiently small to justify the use of an asymptotic expansion in ε. It is obvious that the starting point of the boundary layer approaches the free convection stagnation point as $\varepsilon \to 0$. However, it is worth pointing out that a straightforward expansion is fundamentally unsatisfactory because of its inability to accurately describe the flow in this region. Clearly, a regular expansion fails to be a good approximation no matter how small is ε if we allow x also to become small because the outer stream effects may be dominant in the neighbourhood of the lowest point. So, the scale factors previously adopted become inappropriate in this region. A proper normalization which takes into account the relative importance of the forced convection and which accounts for the mixed convection character of the flow, is therefore needed. It will allow to construct an expansion which adequately approximates the solution near the origin $x = 0$. Following this prominent feature of the local flow, the suitable inner variables are found by making use of the least degeneracy principle. One is led to the following change of variables.

$$x = \varepsilon\tilde{x}, \qquad y = \tilde{y}, \qquad \Psi = \varepsilon\widetilde{\Psi}, \qquad T = \widetilde{T}. \tag{9}$$

In the inner region where the new variables are of order unity, Eqs. (6), (7) become

$$\tilde{L}\widetilde{\Psi}_y - \widetilde{\Psi}_{yyy} - \widetilde{T}\tilde{x} = -\varepsilon \sin\alpha \cos\alpha + \mathrm{O}(\varepsilon^2), \tag{10}$$

$$\mathrm{Pr}\,\tilde{L}\widetilde{T} - \widetilde{T}_{yy} = 0 \tag{11}$$

with the boundary conditions:

$$\widetilde{\Psi}(\tilde{x}, 0) = \Psi_y(\tilde{x}, 0) = 0, \qquad \widetilde{T}(\tilde{x}, 0) = 1, \tag{12}$$

$$\widetilde{\Psi}_y(\tilde{x}, \infty) = -\sin\alpha + \varepsilon\tilde{x}\cos\alpha + \mathrm{O}(\varepsilon^2), \qquad \widetilde{T}(\tilde{x}, \infty) = 0. \tag{13}$$

$\tilde{L}$ is the convective operator $\widetilde{\Psi}_y \partial_{\tilde{x}} - \widetilde{\Psi}_{\tilde{x}} \partial_y$. If we express the solution $(\widetilde{\Psi}, \widetilde{T})$ as power series in ε

$$(\widetilde{\Psi}, \widetilde{T}) = (\widetilde{\Psi}_0, \widetilde{T}_0) + \varepsilon(\widetilde{\Psi}_1, \widetilde{T}_1) + \mathrm{O}(\varepsilon^2) \tag{14}$$

and repeatedly apply the limit process $\varepsilon \to 0$, at $\tilde{x}$ fixed, we obtain at the first two orders the following sequence of problems to be solved in order.

3.1. Zeroth order problem

$$\tilde{L}_0\widetilde{\Psi}_{0y} - \widetilde{\Psi}_{0yyy} - \widetilde{T}_0\tilde{x} = 0, \tag{15}$$

$$\mathrm{Pr}\,\tilde{L}_0\widetilde{T}_0 - \widetilde{T}_{0yy} = 0 \tag{16}$$

with the boundary conditions:

$$\widetilde{\Psi}_0(\tilde{x}, 0) = \widetilde{\Psi}_{0y}(\tilde{x}, 0) = 0, \qquad \widetilde{T}_0(\tilde{x}, 0) = 1, \tag{17}$$

$$\widetilde{\Psi}_{0y}(\tilde{x}, \infty) = -\sin\alpha, \qquad \widetilde{T}_0(\tilde{x}, \infty) = 0, \tag{18}$$

where $\tilde{L}_0$ is obtained from $\tilde{L}$ by substituting $\widetilde{\Psi}_0$ for $\widetilde{\Psi}$.

Note that even at zeroth order, the outer stream effects are taken into account via the driving condition imposed far away from the wall. The problem is then of mixed convection type. Therefore, its solution is more accurate for small x than that of the zeroth order problem we would obtain by a direct expansion without change of variables. In fact, it can be easily verified that the above problem admits an exact solution of the form:

$$\widetilde{\Psi}_0(\tilde{x}, y) = \tilde{x}F_1(y) - \sin\alpha F_0(y), \qquad \widetilde{T}_0(\tilde{x}, y) = G_0(y), \tag{19}$$

F_1, G_0 and F_0 satisfy the two following differential problems:

$$F_1''' + F_1F_1'' - F_1'^2 + G_0 = 0, \tag{20}$$

$$G_0'' + \mathrm{Pr}\,F_1G_0' = 0, \tag{21}$$

$$F_1(0) = F_1'(0) = F_1'(\infty) = G_0(\infty) = 0, \qquad G_0(0) = 1 \tag{22}$$

and

$$F_0''' + F_1F_0'' - F_1'F_0' = 0, \tag{23}$$

$$F_0(0) = F_0'(0) = 0, \qquad F_0'(\infty) = 1, \tag{24}$$

where the primes denote derivatives with respect to the y coordinate.

3.2. First order problem

$$\tilde{L}_0\widetilde{\Psi}_{1y} - \widetilde{\Psi}_{1yyy} + \tilde{L}_1\widetilde{\Psi}_{0y} - \widetilde{T}_1\tilde{x} = -\varepsilon \sin\alpha \cos\alpha, \tag{25}$$

$$\mathrm{Pr}(\tilde{L}_0\widetilde{T}_1 + \tilde{L}_1\widetilde{T}_0) - \widetilde{T}_{1yy} = 0 \tag{26}$$

with the boundary conditions:

$$\widetilde{\Psi}_1(\tilde{x}, 0) = \widetilde{\Psi}_{1y}(\tilde{x}, 0) = 0, \qquad \widetilde{T}_1(\tilde{x}, 0) = 0, \tag{27}$$

$$\widetilde{\Psi}_{1y}(\tilde{x}, \infty) = \tilde{x}\cos\alpha, \qquad \widetilde{T}_1(\tilde{x}, \infty) = 0. \tag{28}$$

It is not difficult to verify that the first order solution resembles the previous one and is written:

$$\widetilde{\Psi}_1(\tilde{x}, y) = \big(\tilde{x}\widetilde{F}_1(y) - \sin\alpha\widetilde{F}_0(y)\big)\cos\alpha, \qquad \widetilde{T}_1(\tilde{x}, y) = \cos\alpha\widetilde{G}_1(y). \tag{29}$$

$\widetilde{F}_1$, $\widetilde{F}_0$ and $\widetilde{G}_1$ are functions of y satisfying the following differential problems:

$$\widetilde{F}_1''' + F_1\widetilde{F}_1'' - 2F_1'\widetilde{F}_1' + F_1''\widetilde{F}_1 + \widetilde{G}_1 = 0, \tag{30}$$

$$\widetilde{G}_1'' + \mathrm{Pr}\big(F_1\widetilde{G}_1' + \widetilde{F}_1G_0'\big) = 0, \tag{31}$$

$$\widetilde{F}_1(0) = \widetilde{F}_1'(0) = \widetilde{G}_1(0) = \widetilde{G}_1(\infty) = 0, \qquad \widetilde{F}_1'(\infty) = 1 \tag{32}$$

and

$$\widetilde{F}_0''' + F_1\widetilde{F}_0'' - F_1'\widetilde{F}_0' = F_0'\widetilde{F}_1' - F_0''\widetilde{F}_1 - 1, \tag{33}$$

$$\widetilde{F}_0(0) = \widetilde{F}_0'(0) = \widetilde{F}_0'(\infty) = 0. \tag{34}$$

It is to be noted that this inner first order solution possesses the remarkable property of being identically zero in the case of cross mixed convection ($\alpha = \pi/2$). Adding the zeroth and first order solutions, we finally get a solution, correct up to $\mathrm{O}(\varepsilon)$ around the stagnation point. Expressed in terms of inner variables, the solution is written:

$$\widetilde{\Psi}(\tilde{x}, y) = \tilde{x}\big(F_1 + \varepsilon\cos\alpha\widetilde{F}_1\big) - \sin\alpha\big(F_0 + \varepsilon\cos\alpha\widetilde{F}_0\big) + \mathrm{O}\big(\varepsilon^2\big), \tag{35}$$

$$T(\tilde{x}, y) = G_0 + \varepsilon\cos\alpha\widetilde{G}_1 + \mathrm{O}\big(\varepsilon^2\big). \tag{36}$$

At this stage, we see that the temperature field and the normal velocity component are determined only by free convection in the particular case $\alpha = \pi/2$ whereas the angular velocity component is of mixed convection type. The latter is however dominated by forced convection as $x \to 0$.

The location x_s of the stagnation point where the wall shear stress vanishes ($\Psi_{yy}(x_s, 0) = 0$) is one of the most important result to come out of the inner solution (35); it is given by:

$$\tilde{x}_s = \frac{x_s}{\varepsilon} = \sin\alpha\frac{F_0''(0) + \varepsilon\cos\alpha\widetilde{F}_0''(0)}{F_1''(0) + \varepsilon\cos\alpha\widetilde{F}_1''(0)} + \mathrm{O}\big(\varepsilon^2\big). \tag{37}$$

4. Outer flow solution

Outside the stagnation zone, a direct numerical integration of Eqs. (1)–(5), complemented by Cauchy's conditions obtained from matching outer and inner solutions, fails to converge in the unfavourable mixed convection domain. This failure would be expected to be a result of the upstream–downstream interaction owing to the occurrence of ascending buoyancy driven flow near the wall and descending flow far away from the wall. This failure also reminds one of the singularity encountered when solving the boundary layer equations near the point of separation. We recall that separation is known to be related physically to the action of an impressed adverse pressure gradient on the boundary layer.

If the pressure is not specified, for example with one other boundary condition for closure, or with an inviscid interacting boundary condition, regular and realistic solutions with reverse flow are obtained by many authors. A key study was that of Catherall and Mangler [15] in which the boundary layer equations were numerically integrated past the point of zero skin friction in a nonsingular manner by allowing the pressure to be an unknown function which was determined as a part of the solution. However, in this coupling approach Prandtl's equations are no longer parabolic since upstream influence is possible by means of an unknown closure boundary condition. In order to take into account the ellipticity of the problem in the unfavourable mixed convection region and so to avoid numerical divergence, the iterative procedure, hereafter described, is used. We have first to define a free curve $y = Y(x)$ along which the velocity component u vanishes and on each side of which u keeps the same sign: $\mathrm{Sgn}(u) = \mathrm{Sgn}(Y - y)$. In the region near the wall ($0 < y < Y$) the initial boundary value problem (1)–(5) is solved numerically by using a second order implicit finite difference scheme; the integration is performed by increasing x from an arbitrarily specified station in the inner domain (the stagnation point x_s for instance) until the station $x = \alpha$. It is to be noted that this problem is solved globally without using expansion procedure, then its solution is also valid in the inner domain. Furthermore, the inner solution is calculated independently of the remainder of the flow field. For these reasons the outer solution can simply be initialized by continuity using the inner solution at the stagnation point. This type of matching is obviously consistent with the steps of the classical matched asymptotic expansions.

In the region ($Y < y < \infty$), the problem is solved by decreasing x from $x = \alpha$ until the stagnation point where the resulting solution must be compatible with the inner solution. The approximate corresponding initial values are sought by performing a

local perturbation expansion with respect to ε. At zeroth order in ε, the flow is governed by free convection; the corresponding solution vanishes asymptotically for sufficiently large y, say for $y > \delta_n(x)$, $\delta_n(x)$ being the local free convection boundary layer thickness. At first order in ε and out of the free convection boundary layer, it is easy to obtain that: $u_1(x, y) = u_e(x)$ and $T_1(x, y) = 0$. Therefore, by taking $x = \alpha$ and by neglecting second order terms in ε we get:

$$u(\alpha, y) = T(\alpha, y) = \frac{\partial T}{\partial x}(\alpha, y) = 0 \quad \text{and} \quad \frac{\partial u}{\partial x}(\alpha, y) = \varepsilon \quad \text{for } y > \delta_n(x).$$

Solving these two problems requires however the specification of the temperature $T(x, Y(x))$ along the free curve, say $\theta(x)$. We can accordingly consider the dependent variables u, v and T as functionals of Y and θ. The dependence of these functional on Y and θ is however not explicit in the sense that it is realized by solving two initial boundary value problems. We note that the calculated variables u, v and T are naturally continuous along the curve $(x, Y(x))$. This property yields the continuity of their tangential derivatives and hence that of the normal derivative of v in accordance with the continuity equation. So, only the normal derivatives of u and T must be continuous along the correct free curve in order that the closure of the problem be ensured. Instead of the continuity of the previous normal derivatives, it is equivalent and more convenient to express the closure conditions in terms of the radial derivatives of u and T, namely:

$$\left[\frac{\partial T}{\partial y}\right]_{Y(x)} = \left[\frac{\partial u}{\partial y}\right]_{Y(x)} = 0, \tag{38}$$

where $[f]$ denotes the jump of the quantity f across the free curve $y = Y(x)$.

Satisfying these two conditions requires the use of an iterative process to calculate a set of functions Y_n and θ_n which must converge towards the equilibrium state (Y, θ). A possible disadvantage of such an iteration process is that if more than a few iterations are required for convergence, then the method becomes inefficient. In order to overcome this possible disadvantage, the predicted functions $Y_n(x)$ and $\theta_n(x)$ are patched by means of variational boundary and initial value problems which are defined from the problems to be solved on either side of the free curve. When the equilibrium state is reached then any infinitesimal change

$$Y_n(x) \to Y_{n+1}(x) = Y_n(x) + e\delta Y_n(x), \tag{39}$$

$$\theta_n(x) \to \theta_{n+1}(x) = \theta_n(x) + e\delta\theta_n(x) \tag{40}$$

not altering the fixed end points ($\delta Y(\alpha) = \delta Y(x_s) = \delta\theta(\alpha) = \delta\theta(x_s) = 0$) should have no effects on the functionals

$$J_1(Y, \theta) = \left[\frac{\partial u}{\partial y}\right]_{Y(x)} \quad \text{and} \quad J_2(Y, \theta) = \left[\frac{\partial T}{\partial y}\right]_{Y(x)}. \tag{41}$$

This means that $\delta J_1 = \delta J_2 = 0$. So, the problem amounts to finding the extrema of the functional J_1 and J_2. The calculation for determining accurately the previous sequence of near identity transformations is then done on the lines of the classical calculus of variations. Assuming that small changes in Y and θ yield small variations in the solution (u, T), then we can write:

$$u_{n+1} = u_n + e\delta u_n, \qquad \theta_{n+1} = \theta_n + e\delta\theta_n, \tag{42}$$

where (u_n, T_n) is the vector field solution corresponding to the conditions:

$$u_n\big(x, Y_n(x)\big) = 0, \quad T_n\big(x, Y_n(x)\big) = \theta_n(x), \quad n = 0, 1, \ldots. \tag{43}$$

It is to be noted that the variation δu_n and δT_n satisfy the following homogeneous boundary conditions:

$$\delta u_n(x, 0) = \delta u_n(x, \infty) = 0, \qquad \delta T_n(x, 0) = \delta T_n(x, \infty) = 0. \tag{44}$$

So, at any point of the flow, it comes down to saying that the variations $\delta u_n(x, y)$ and $\delta T_n(x, y)$, resulting only from the deformations of the free curve and the change of the specified temperature on it, are due to the boundary values $\delta u_n(x, Y_n)$ and $\delta T_n(x, Y_n)$. Once we make the following change of notations:

$$U = u_n(x, Y_n), \qquad \delta U = \delta u_n(x, Y_n), \tag{45}$$

$$\tau = T_n(x, Y_n), \qquad \delta\tau = \delta T_n(x, Y_n), \tag{46}$$

$$u(x, y) = \tilde{u}(U, \tau), \qquad T(x, y) = \widetilde{T}(U, \tau) \tag{47}$$

we can write

$$\delta u_n(x, y) = \frac{\partial \tilde{u}}{\partial U}\delta U + \frac{\partial \tilde{u}}{\partial \tau}\delta\tau, \tag{48}$$

$$\delta T_n(x, y) = \frac{\partial \widetilde{T}}{\partial U}\delta U + \frac{\partial \widetilde{T}}{\partial \tau}\delta\tau, \tag{49}$$

where $\partial\tilde{u}/\partial U$, $\partial\tilde{u}/\partial\tau$, $\partial\widetilde{T}/\partial U$ and $\partial\widetilde{T}/\partial\tau$ indicate functional derivatives which will be calculated later, using the formal definitions:

$$\delta U\frac{\partial\tilde{u}}{\partial U}=\left.\frac{\mathrm{d}}{\mathrm{d}e}\right|_{e=0}\tilde{u}(U+e\delta U,\tau), \tag{50}$$

$$\delta\tau\frac{\partial\tilde{u}}{\partial\tau}=\left.\frac{\mathrm{d}}{\mathrm{d}e}\right|_{e=0}\tilde{u}(U,\tau+e\delta\tau). \tag{51}$$

Analogous expressions hold for $\widetilde{T}$ instead of $\tilde{u}$.

By setting $\delta U=\delta\tau=1$ in (50), (51), one obtains

$$\frac{\partial\tilde{u}}{\partial U}=\left.\frac{\mathrm{d}}{\mathrm{d}e}\right|_{e=0}\tilde{u}(U+e,\tau),\qquad \frac{\partial\tilde{u}}{\partial\tau}=\left.\frac{\mathrm{d}}{\mathrm{d}e}\right|_{e=0}\tilde{u}(U,\tau+e). \tag{52}$$

Similar relations take place by substituting $\widetilde{T}$ for $\tilde{u}$, namely

$$\frac{\partial\widetilde{T}}{\partial U}=\left.\frac{\mathrm{d}}{\mathrm{d}e}\right|_{e=0}\widetilde{T}(U+e,\tau),\qquad \frac{\partial\widetilde{T}}{\partial\tau}=\left.\frac{\mathrm{d}}{\mathrm{d}e}\right|_{e=0}\widetilde{T}(U,\tau+e). \tag{53}$$

The previous functional derivatives are calculated in the flow field by solving two appropriate variational problems on either side of the curve $y=Y_n(x)$. The governing equations are found by performing variational differentiation of Eqs. (1)–(3) with respect to the function U and τ. Thus:

(a) by differentiation with respect to U one obtains

$$\frac{\partial}{\partial x}\left(\frac{\partial\tilde{u}}{\partial U}\right)_n+\frac{\partial}{\partial y}\left(\frac{\partial\tilde{v}}{\partial U}\right)_n=0, \tag{54}$$

$$\left(\frac{\partial u_n}{\partial x}+u_n\frac{\partial}{\partial x}+v_n\frac{\partial}{\partial y}-\frac{\partial^2}{\partial y^2}\right)\left(\frac{\partial\tilde{u}}{\partial U}\right)_n+\frac{\partial u_n}{\partial y}\left(\frac{\partial\tilde{v}}{\partial U}\right)_n=\left(\frac{\partial\widetilde{T}}{\partial U}\right)_n\sin x, \tag{55}$$

$$\left(u_n\frac{\partial}{\partial x}+v_n\frac{\partial}{\partial y}-\frac{1}{\mathrm{Pr}}\frac{\partial^2}{\partial y^2}\right)\left(\frac{\partial\widetilde{T}}{\partial U}\right)_n+\frac{\partial T_n}{\partial x}\left(\frac{\partial\tilde{u}}{\partial U}\right)_n+\frac{\partial T_n}{\partial y}\left(\frac{\partial\tilde{v}}{\partial U}\right)_n=0. \tag{56}$$

The corresponding boundary and initial conditions, which can be readily deduced from (52), (53) are as follow:

$$\frac{\partial\tilde{u}}{\partial U}=1,\quad \frac{\partial\widetilde{T}}{\partial U}=0\quad \text{for } y=Y_n, \tag{57}$$

$$\frac{\partial\tilde{u}}{\partial U}=\frac{\partial\widetilde{T}}{\partial U}=0\quad \text{for } y=0 \text{ and } y\to\infty, \tag{58}$$

$$\frac{\partial\tilde{u}}{\partial U}=\frac{\partial\widetilde{T}}{\partial U}=0,\qquad \frac{\partial}{\partial\mathrm{x}}\left(\frac{\partial\tilde{u}}{\partial U}\right)=\frac{\partial}{\partial\mathrm{x}}\left(\frac{\partial\widetilde{T}}{\partial U}\right)=0\quad \text{for } x=x_s \text{ and } x=\alpha; \tag{59}$$

(b) by differentiation with respect to τ one obtains

$$\frac{\partial}{\partial x}\left(\frac{\partial\tilde{u}}{\partial\tau}\right)_n+\frac{\partial}{\partial y}\left(\frac{\partial\tilde{v}}{\partial\tau}\right)_n=0, \tag{60}$$

$$\left(\frac{\partial u_n}{\partial x}+u_n\frac{\partial}{\partial x}+v_n\frac{\partial}{\partial y}-\frac{\partial^2}{\partial y^2}\right)\left(\frac{\partial\tilde{u}}{\partial\tau}\right)_n+\frac{\partial u_n}{\partial y}\left(\frac{\partial\tilde{v}}{\partial\tau}\right)_n=\left(\frac{\partial\widetilde{T}}{\partial\tau}\right)_n\sin x, \tag{61}$$

$$\left(u_n\frac{\partial}{\partial x}+v_n\frac{\partial}{\partial y}-\frac{1}{\mathrm{Pr}}\frac{\partial^2}{\partial y^2}\right)\left(\frac{\partial\widetilde{T}}{\partial\tau}\right)_n+\frac{\partial T_n}{\partial x}\left(\frac{\partial\tilde{u}}{\partial\tau}\right)_n+\frac{\partial T_n}{\partial y}\left(\frac{\partial\tilde{v}}{\partial\tau}\right)_n=0. \tag{62}$$

These equations are subject to the boundary conditions

$$\frac{\partial\tilde{u}}{\partial\tau}=0,\quad \frac{\partial\widetilde{T}}{\partial\tau}=1\quad \text{for } y=Y_n, \tag{63}$$

$$\frac{\partial\tilde{u}}{\partial\tau}=\frac{\partial\widetilde{T}}{\partial\tau}=0\quad \text{for } y=0 \text{ and } y\to\infty \tag{64}$$

and homogeneous initial conditions similar to (59).

Eqs. (54)–(56) and (60)–(62) together with their respective associated boundary and initial conditions are solved numerically by using a classical second order implicit difference scheme. Now that the functional derivatives have been computed, we turn to the expression (48), (49) which must be used together with the stationary conditions (38) to clarify the iterative procedure. First of all, we must express the variations $\delta u_n(x, y)$ and $\delta T_n(x, y)$ in terms of $\delta\theta$ and δY instead of δU and $\delta\tau$. For this, we recall that $u_n(x, Y_n) = 0$ and $u_{n+1}(x, Y_{n+1}) = 0$. By using a Taylor expansion and keeping only the leading term, we obtain from (39), (42) and (45):

$$\delta U = -\frac{\partial u_n}{\partial y}\delta Y. \tag{65}$$

In the same way, since $T_n(x, Y_n) = \theta_n$ and $T_{n+1}(x, Y_{n+1}) = \theta_{n+1}$, we get by subtraction:

$$\delta\tau = \delta\theta - \frac{\partial T_n}{\partial y}\delta Y. \tag{66}$$

Expressions (48), (49) become then:

$$\delta u_n(x, y) = \left(\frac{\partial\tilde{u}}{\partial\tau}\right)_n \delta\theta - \left\{\left(\frac{\partial\tilde{u}}{\partial U}\right)_n \frac{\partial u_n}{\partial y} + \left(\frac{\partial\tilde{u}}{\partial\tau}\right)_n \frac{\partial T_n}{\partial y}\right\}\delta Y, \tag{67}$$

$$\delta T_n(x, y) = \left(\frac{\partial\widetilde{T}}{\partial\tau}\right)_n \delta\theta - \left\{\left(\frac{\partial\widetilde{T}}{\partial U}\right)_n \frac{\partial u_n}{\partial y} + \left(\frac{\partial\widetilde{T}}{\partial\tau}\right)_n \frac{\partial T_n}{\partial y}\right\}\delta Y. \tag{68}$$

Transforming (38) in view of (39) and (42) gives:

$$\left[\frac{\partial u_n}{\partial y} + \frac{\partial^2 u_n}{\partial y^2}\delta Y + \frac{\partial}{\partial y}(\delta u_n)\right]_{Y_n(x)} = 0, \tag{69}$$

$$\left[\frac{\partial T_n}{\partial y} + \frac{\partial^2 T_n}{\partial y^2}\delta Y + \frac{\partial}{\partial y}(\delta T_n)\right]_{Y_n(x)} = 0. \tag{70}$$

Making use of the linear forms (67), (68), the constraints (69), (70) become:

$$\left[\frac{\partial T_n}{\partial y}\right]_{Y_n} + \left[\frac{\partial}{\partial y}\left(\frac{\partial\widetilde{T}}{\partial\tau}\right)_n\right]_{Y_n(x)}\delta\theta + \left[\frac{\partial^2 T_n}{\partial y^2} - \frac{\partial}{\partial y}\left\{\left(\frac{\partial\widetilde{T}}{\partial U}\right)_n \frac{\partial u_n}{\partial y} + \left(\frac{\partial\widetilde{T}}{\partial\tau}\right)_n \frac{\partial T_n}{\partial y}\right\}\right]_{Y_n(x)}\delta Y = 0, \tag{71}$$

$$\left[\frac{\partial u_n}{\partial y}\right]_{Y_n} + \left[\frac{\partial}{\partial y}\left(\frac{\partial\tilde{u}}{\partial\tau}\right)_n\right]_{Y_n(x)}\delta\theta + \left[\frac{\partial^2 u_n}{\partial y^2} - \frac{\partial}{\partial y}\left\{\left(\frac{\partial\tilde{u}}{\partial U}\right)_n \frac{\partial u_n}{\partial y} + \left(\frac{\partial\tilde{u}}{\partial\tau}\right)_n \frac{\partial T_n}{\partial y}\right\}\right]_{Y_n(x)}\delta Y = 0. \tag{72}$$

These two relations allow us to calculate the increments $\delta\theta$ and δY at each step of the iterative procedure. A summary is now given of the iterative procedure which was used to solve the outer problem.

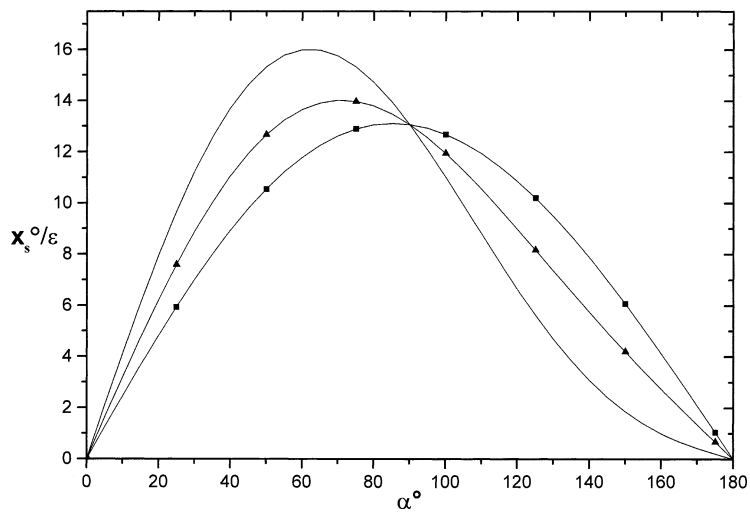

Fig. 2. Stagnation point position as function of α for various ε (—■—) $\varepsilon = 0.01$; (—▲—) $\varepsilon = 0.05$; (——) $\varepsilon = 0.1$.

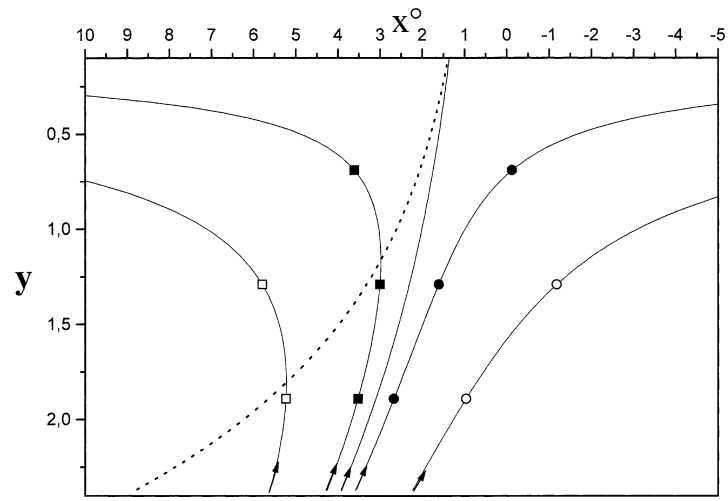

Fig. 3. Stagnation point streamlines (—○—) $\Psi = -0.025$; (—●—) $\Psi = -0.005$; (——) $\Psi = 0$; (—■—) $\Psi = 0.005$; (—□—) $\Psi = 0.025$; (- - -) $u = 0$.

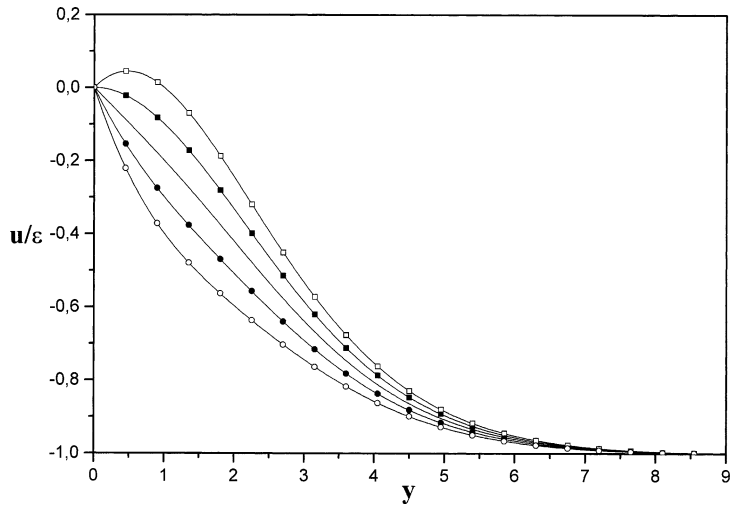

Fig. 4. Velocity profiles near the stagnation point (—○—) $x = -2x_s$; (—●—) $x = -x_s$; (——) $x = 0$; (—■—) $x = x_s$; (—□—) $x = 2x_s$.

(i) The procedure begins by the choice of an initial approximation $y = Y_0(x)$ of the free curve. A straight line joining the stagnation point $(x_s, 0)$ and the point $(\alpha, \delta_n(\alpha))$ serves to this initialization. Along this curve a linear temperature distribution $\theta(x) = (x - \alpha)/(x_s - \alpha)$ is prescribed. The inner solution is then used to start the numerical integration.
(ii) Solve Eqs. (6)–(8) firstly by increasing x from x_s until $x = \alpha$ and secondly by decreasing x from $x = \alpha$ to $x = x_s$.
(iii) Repeat the step (ii) for solving Eqs. (54)–(56) and (60)–(62).
(iv) Calculate increments $\delta\theta(x)$ and $\delta Y(x)$ using (71), (72) and new estimates for $Y(x)$ and $\theta(x)$ using (39), (40).
(v) Return to step (ii) and repeat the procedure until the maximum jumps $[\partial T/\partial y]_{Y(x)}$ and $[\partial u/\partial y]_{Y(x)}$ become sufficiently small, within a prescribed tolerance.

5. Some numerical results

The following numerical experiments are performed for $\mathrm{Pr} = 0.72$. The iterative Newton's method associated to a fourth order Runge Kutta scheme is used to solve the differential problems involving the different functions which serve to construct the inner solution. First of all, we give in Fig. 2 the location of the stagnation point as a function of the inclination α for some values of ε. It is interesting to observe that the maximum value of x_s/ε is not attained at $\alpha = \pi/2$ for fixed ε; this occurs only in the limit $\varepsilon \to 0$.

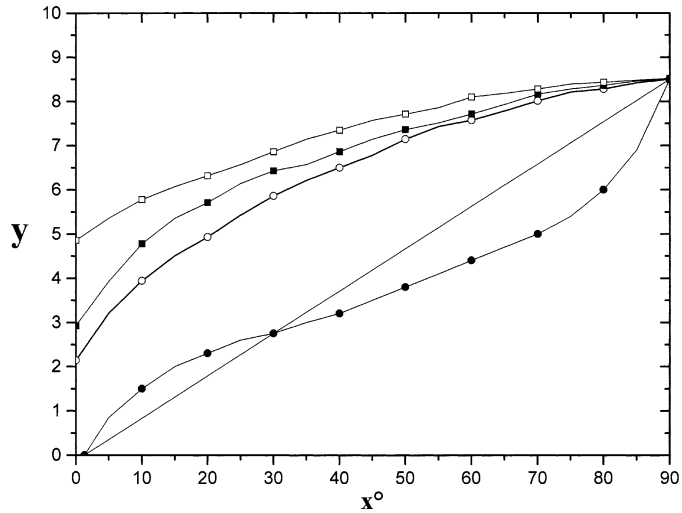

Fig. 5. Contours $u = 0$: (——) initial approximation $Y_0(x)$; (—●—) equilibrium position $Y(x)$. Boundary layer thickness: (—○—) symmetric convection; (—■—) free convection; (—□—) asymmetric convection.

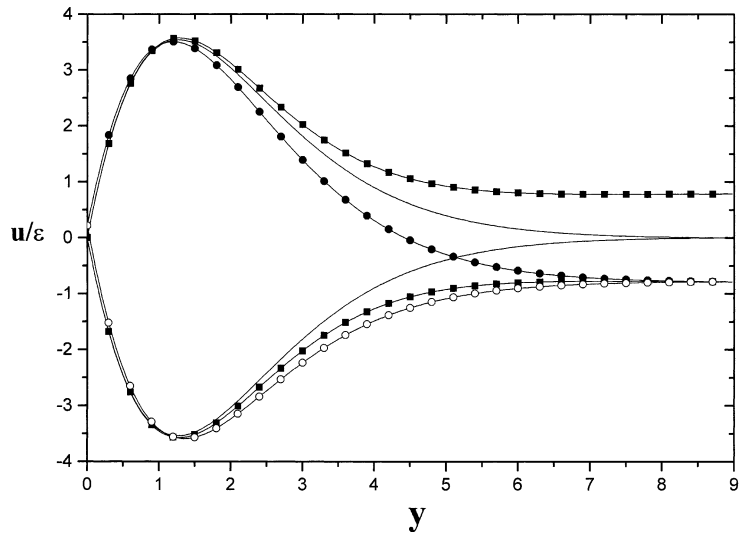

Fig. 6. Velocity profiles: free convection (——) and symmetric convection (—■—) at $x = \mp\pi/4$; asymmetric convection at $x = \pi/4$ (—●—) and $x = -\pi/4$ (—○—).

Since the flow in the region between the stagnation points of free and forced convection is expected to be qualitatively similar for all sufficiently small, fixed ε and all α in the range $(0, \pi)$, only the values $\varepsilon = 0.1$ and $\alpha = \pi/2$ are considered in illustrating the numerical results. The streamlines shown in Fig. 3 give an overall picture of the flow in the magnified inner domain where the radial coordinate as well as the arc length along the cylinder are referred to $R\mathrm{Gr}^{-1/4}$. This means that both x and y are enlarged by a factor $\mathrm{Gr}^{1/4}$. In this unit, y is of order unity whereas x becomes sufficiently large for being plotted along a straight axis. In this region, the structure of the flow resembles that of the flow occurring near a reattachment point. A reverse flow appears from the stagnation point of abscissa x_s where buoyancy forces are just equilibrated by the outer flow effects. Near the wall, the flow sense is imposed either by buoyancy forces for $x > x_s$ or by outer stream effects for $x < x_s$. The dividing streamline $\Psi = 0$ is analogous to a separation line of a separated boundary layer, while the curve $u = 0$ divides the reverse flow domain into two regions, each dominated by either forced or free convection. Near the wall, the flow is upward and is governed mainly by free convection whereas forced convection effects are more important far from the wall. In agreement with this, the curve $u = 0$ is the set of turning points of the inner streamlines.

In Fig. 4, we have plotted angular velocity profiles as functions of the normal coordinate for different abscissa. It is to be noted that, for small x ($|x| < x_s$), the flow direction is rather imposed by the outer flow. As $|x|$ increases, the free convection

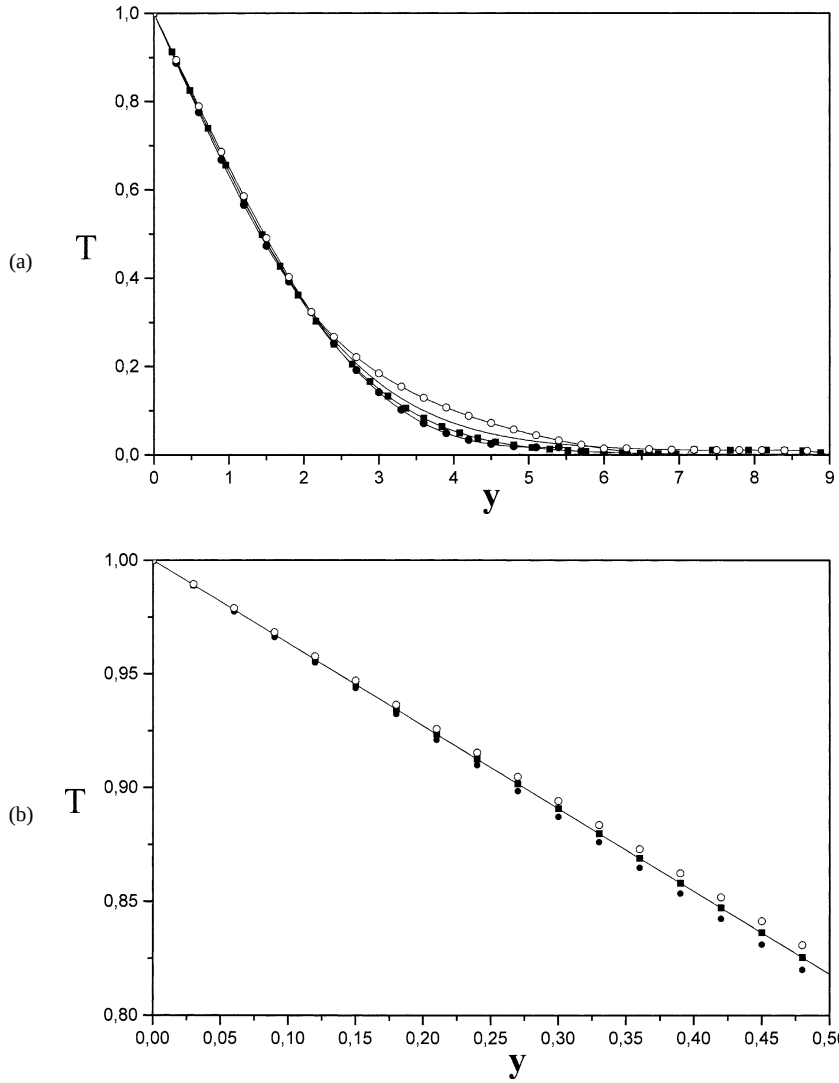

Fig. 7. (a) Temperature profiles: free convection (——) and symmetric convection (—■—) at $x = \mp\pi/4$; asymmetric convection at $x = \pi/4$ (—●—) and $x = -\pi/4$ (—○—). (b) Enlarged Fig. 7(a) near the wall.

becomes more and more significant while the forced convection less and less important. For this reason, one can see a positive velocity near the wall for $x > x_s$. The asymmetry between the profiles occurring at positive and negative abscissas illustrates the importance of the forced convection perturbation in the vicinity of the free convection stagnation point.

Outside the stagnation zone, the iterative method described previously is used to solve separately the whole problem (6)–(8) on both sides of the free curve along which $u = 0$. The procedure is associated to a classical second order finite difference scheme. The numerical efficiency of the algorithm (stability and rate of convergence) was found satisfactory. The equilibrium state is reached after only a few iterations, about ten iterations for a tolerance test of 10^{-3}. A simple illustration of the consistency of the foregoing method is provided by the fact that the initial condition for the boundary layer problem in the region $0 < y < Y(x)$ is retrieved, within $O(\varepsilon^2)$, as a result of the calculation in the region $Y(x) < y < \infty$).

For comparison, we show in Fig. 5 the curves along which $u = 0$ at the initial stage of the iterative procedure ($y = Y_0(x)$) and when the equilibrium state is reached ($y = Y(x)$) together with the boundary layer thickness corresponding to free convection, symmetric and asymmetric mixed convections (the boundary layer thickness is defined here as the distance from the wall beyond which the difference $u - u_e$ vanishes within a tolerance test of 10^{-2}); this definition is chosen in accordance with the accuracy $O(\varepsilon^2)$ of the calculation. A more accurate definition should have no significant effect on the numerical results. Note that the free convection boundary layer thickness is greater than that of symmetric mixed convection and less than that of asymmetric mixed convection. The discrepancies are however of order ε.

To illustrate how the forced convection affects the free convection boundary layer flow, representative velocity profiles at $x = \pm\pi/4$ are shown in Fig. 6. As a result of the flow asymmetry, the velocity gradient at the wall increases for aiding flow and decreases in the opposite mixed convection region. This is respectively accompanied by higher and smaller boundary layer velocities. Fig. 7(a) depicts temperature profiles at the same locations; their difference and the comparison with the purely free convection case indicate that heat transfer is enhanced when buoyancy aids motion (symmetric case and asymmetric case at $x = -\pi/4$) and is reduced in the opposite case ($x = \pi/4$). Fig. 7(b) represents enlarged temperature profiles in the neighbourhood of the wall in order to better show the influence of the free stream on the local heat transfer.

6. Concluding remarks

A free convection boundary layer perturbed by a transverse stream around a heated circular cylinder is investigated. Whereas obvious Cauchy conditions, deduced by symmetry of the governing equations, are associated with the symmetric mixed convection problem, the asymmetric case has no trivial Cauchy conditions because of the downstream–upstream interaction occurring in the opposite mixed convection domain. In the limiting case of small forced convection effects, a semi-analytical solution is found near the free convection stagnation point. This solution allows us to retrieve approximate Cauchy conditions and accounts for the particular local structure of the flow. The latter is then extended outside the stagnation zone by solving the whole problem by a direct second order numerical method in the favourable mixed convection domain. This procedure however fails to converge in the opposite mixed convection domain. In order to avoid numerical divergence owing to the existence of reverse flow, an iterative method which takes into account the flow direction is implemented. The procedure works primarily by seeking the boundary curve separating the upstream and downstream flows. It is based upon a variational method which consists of calculating the extremal of the jumps of the radial derivatives of the temperature and the angular velocity component along the free curve. In this way, the equilibrium state is reached with only a few iterations.

Acknowledgements

The authors would like to sincerely thank the referees for their helpful comments and suggestions.

References

[1] N.D. Joshi, S.P. Sukatme, An analysis of combined free and forced convection heat transfer from a horizontal circular cylinder to a transverse flow, J. Heat Transfer 93 (1971) 441–448.
[2] E.M. Sparrow, L. Lee, Analysis of mixed convection about a horizontal cylinder, Int. J. Heat Mass Transfer 19 (1976) 229–231.
[3] J.H. Merkin, Mixed convection from horizontal circular cylinder, Int. J. Heat Mass Transfer 20 (1977) 73–76.
[4] W.W. Wood, Free and forced convection from fine hot wires, J. Fluid Mech. 55 (3) (1972) 419–438.
[5] S. Nakai, T. Okazaki, Heat transfer from horizontal circular wire at small Reynolds and Grashof numbers. II: Mixed convection, Int. J. Heat Mass Transfer 18 (1975) 397–413.
[6] H.M. Badr, Laminar mixed convection from a horizontal cylinder, parallel and contra flow regimes, Int. J. Heat Mass Transfer 27 (1984) 17–27.
[7] B. Sunden, Influence of buoyancy forces and thermal conductivity on flow field and heat transfer of circular cylinders at small Reynolds numbers, Int. J. Heat Mass Transfer 26 (9) (1983) 1329–1338.
[8] H.M. Badr, On the effect of flow direction on mixed convection from a horizontal cylinder, Int. J. Numer. Methods Fluids 5 (1985) 1–12.
[9] M. Amaouche, J.L. Peude, Convection mixte stationnaire autour d'un cylindre horizontal, Int. J. Heat Mass Transfer 28 (7) (1985) 1269–1279.
[10] A.P. Hatton, D.D. Tames, H.W. Swire, Combined forced and free convection with low speed air flow over horizontal cylinder, J. Fluid Mech. 42 (1) (1969) 17–31.
[11] G.K. Sharma, S.P. Sukhtame, Combined free and forced convection heat transfer from a heated tube to a transverse air stream, J. Heat Transfer 91 (1969) 457–459.
[12] P.H. Oostuizen, S. Madan, The effect of flow direction on combined convective heat transfer cylinders to air, J. Heat Transfer 93 (1971) 240–242.
[13] M. Amaouche, On some mixed convection flows described by exact solutions of Prandtl equations, Eur. J. Mech. B Fluids, 10 (3) (1991) 295–312.
[14] M. Amaouche, C. Nouar, Calcul au second ordre d'une couche limite de convection mixte, Int. J. Heat Mass Transfer 36 (10) (1993) 2702–2706.
[15] K.W. Catherall, D. Mangler, The integration of two dimensional laminar boundary layer equations past the point of vanishing skin friction, J. Fluid Mech. 26 (1966) 163–175.